Estuaries and Coasts
https://doi.org/10.1007/s12237-022-01131-4

SPECIAL ISSUE: WETLAND ELEVATION DYNAMICS

Comparing Vertical Change in Riverine, Bayside, and Barrier Island Wetland Soils in Response to Acute and Chronic Disturbance in Apalachicola Bay, FL

Havalend E. Steinmuller[1,3,4] · Ethan Bourque[2] · Samantha B. Lucas[2] · Kevin M. Engelbert[1] · Jason Garwood[2] · Joshua L. Breithaupt[1]

Received: 26 May 2022 / Revised: 31 August 2022 / Accepted: 28 September 2022

Abstract
Coastal wetlands experience acute and chronic disturbances which can affect rates of surface elevation change and vertical accretion of surface sediments. Disturbance can either amplify or impair the ability of wetlands to maintain their position within the tidal frame, with implications for their long-term persistence. Using an 8-year dataset collected from coupled surface elevation table-marker horizon (SET-MH) stations spanning riverine, bayside, and barrier island settings in the Apalachicola Bay region of north Florida, USA, this study investigated decadal-scale surface elevation change and vertical accretion rates to assess wetland vulnerability to acute (Hurricane Michael) and chronic (relative sea-level rise; RSLR) disturbance in different geomorphic settings. All sites had long-term accretion rates that exceeded rates of surface elevation change (pre-Michael), indicating that surface accretion was not a good indicator of changes in surface elevation for any of these coastal geomorphic settings. Hurricane Michael increased surface elevation change rates at bayside and riverine sites; barrier island sites consistently displayed the lowest surface elevation change rates, which did not differ between pre- and post-Michael periods. Accretion rates were greatest in the riverine sites, which were characterized by highly organic soils. Barrier island and bayside sites demonstrated elevation and accretion deficits relative to the rate of RSLR for Apalachicola Bay between 2010 and 2022, indicating high vulnerability of these sites to chronic increases in sea level. These estimates of marsh resilience relied exclusively on rates of vertical change and neglecting to account for lateral erosion failed to predict that each of the three barrier island sites experienced rapid loss of the seaward SET-MH stations during the observation period. These results provide evidence of different vertical change responses among coastal wetlands of three geomorphic settings exposed to hurricanes and RSLR in the same region and suggest different timelines for long-term persistence of these sites.

Keywords Surface elevation · Accretion · SET-MH · Coastal wetland · Geomorphic setting · Gulf Coast

Introduction

Elevation in coastal wetlands is a function of both surface and subsurface hydrologic and biologic processes that work interactively to control material input and output as well as soil volume changes (Cahoon et al. 2006). Material input can occur through sediment deposition (Morris et al. 2002; Stone and Walling 1997; Cahoon et al. 2006), accumulation of organic material at the soil surface (Cahoon et al. 2006), and subsurface root production (McKee et al. 2007). These inputs are counterbalanced by scouring and erosion, root mortality, decomposition, and potential export of degradation products (Morris et al. 2002; Cahoon et al. 2006, McKee et al. 2007). Soil volume changes, which include autocompaction and dilation, can also alter the elevation of coastal

Communicated by Charles T. Roman

✉ Havalend E. Steinmuller
hsteinmuller@disl.org

1 Coastal and Marine Laboratory, Florida State University, St. Teresa, FL, USA

2 Apalachicola National Estuarine Research Reserve, Florida Department of Environmental Protection, Eastpoint, FL, USA

3 Dauphin Island Sea Lab, Dauphin Island Sea Lab, AL, USA

4 School of Marine & Environmental Sciences, University of South Alabama, Mobile, AL, USA

Published online: 26 October 2022

wetlands (Kaye and Barghoorn 1964; Nuttle et al. 1990; Whelan et al. 2005). Quantification of changes to surface elevation requires either direct quantification of individual biological, hydrological, and geological processes, or the measurement of the cumulative effects of these processes over long timescales (5+ years) (Cahoon et al. 2002; Webb et al. 2013). The coupled surface elevation table-marker horizon (SET-MH) method provides the ability to conduct long-term measurements of cumulative surface elevation change in coastal wetlands and has been utilized globally to compare trends and drivers of change in surface elevation (Cahoon et al. 2002; Callaway et al. 2013; Stagg et al. 2013; Raposa et al. 2016; Osland et al. 2017; Cahoon et al. 2020).

Globally, the acceleration of sea-level rise (SLR) threatens the extent of coastal wetlands (Church and White 2006; Dangendorf et al. 2019). Coastal wetland systems respond to this chronic disturbance by developing vertically via surface accretion or sub-surface root-zone expansion, transgressing landwards to track changes in the physicochemical environment that constrain productivity, or through submergence and conversion to open water (Reed 1995). These three scenarios are regulated by a variety of site-specific factors, the most important of which are the rate of sea-level rise (SLR) relative to the tidal frame, available space for wetlands to transgress landwards, and sediment supply (Spencer et al. 2016). With only an estimated 37% of global coastal wetlands having available space to transgress landwards (Schuerch et al. 2018), vertical development of the soil surface becomes a key element for determining the vulnerability of wetlands to SLR (Morris et al. 2002; Cahoon et al. 2006; Webb et al. 2013).

In addition to the chronic disturbance of SLR, coastal wetlands are also subject to periodic acute disturbances, such as hurricanes. These high-intensity, low-frequency events can cause extensive effects on ecosystem processes and characteristics that persist over variable timescales (Paerl et al. 2001; Danielson et al. 2017; Cahoon et al. 2003). Hurricanes can cause extensive vegetation dieback (Stagg et al. 2021; Osland et al. 2020) and defoliation (Danielson et al. 2017), as well as catalyze abrupt changes in vertical development of the soil surface. Elevation loss can occur through hurricane-associated erosion and root zone collapse, while elevation gain occurs through deposition (Breithaupt et al. 2019; Baustian and Mendelssohn 2015; Cahoon et al. 2006; Feher et al. 2020; McKee and Cherry 2009; Moon et al. 2022; Yeates et al. 2020). The impacts of hurricanes on vertical development of the soil surface are critical to understand in the face of increasing frequency of intense hurricanes and increased rainfall associated with hurricanes as a result of climate change (Seneviratne et al. 2021), with implications for forecasting and characterizing marsh vulnerability.

Classification of coastal wetland types allows for differentiation of complex environmental factors that constrain ecological processes (Lugo and Snedaker 1974; Thom 1982; Brinson 1993; Woodroffe 1993; Selvam 2003; Cahoon et al. 2006; Dürr et al. 2011). Specifically, coastal wetlands can be classified by geomorphic setting, which has previously been demonstrated as a predictor for various wetland functions and characteristics, including soil stoichiometry, soil carbon stocks, soil organic matter accumulation, sedimentation rates, and marsh elevation dynamics (Adame et al. 2010; Haaf et al. 2022; Rovai et al. 2018; Twilley et al. 2018). The goal of this study was to determine how marsh elevation dynamics of coastal wetlands in three geomorphic settings differ in response to regional-scale disturbances. Specifically, we investigated decadal-scale surface elevation change and vertical accretion rates to assess vulnerability of bayside, riverine, and barrier island wetlands to acute (hurricane incidence) and chronic (SLR) disturbance. These three geomorphic settings span a gradient of estuarine position, tidal regime, and sediment supply (Light et al. 1998; Edmiston 2008). We hypothesized that the riverine wetlands would have the greatest rates of elevation change and accretion and would be most resilient to relative SLR, due to their closer proximity to sediment sources and freshwater inputs (Haaf et al. 2022). Bayside and barrier island wetlands were expected to demonstrate surface elevation change and accretion rates similar to each other and to RSLR rates (Cahoon et al. 2006), as we expected vertical processes at these sites to be dominated more by RSLR and accommodation space than riverine processes (Cahoon et al. 2006; Breithaupt et al. 2018; Kirwan and Megonigal 2013). We expected an increase in elevation and accretion rates associated with the landfall of Hurricane Michael, though the magnitude and persistence of this increase was expected to differ between geomorphic settings.

Methods

Site Description

The Apalachicola Bay estuary, located in the northeastern panhandle of Florida, contains coastal wetlands of multiple geomorphic settings and provides a unique setting to compare the effects of acute and chronic disturbance on wetland surface elevation (Fig. 1). The Apalachicola River is highly managed by a series of reservoirs and dams in Georgia and Alabama, which have contributed to a decline in water levels over the last 50 years (Light et al. 1998; Mossa et al. 2017). The combination of local erosion of the river channel and decreased spring and summer flows have caused an increased incidence of severe drought conditions, which generally occur between April and August (Darst and Light 2008). These drought conditions have resulted in a desiccation of floodplain forests (Darst and Light 2008), altered species compositions in forested wetlands (Light et al. 1998; Darst and Light 2008; Stallins et al. 2010; Smith 2013), and decreases in sediment supply to estuarine wetlands located

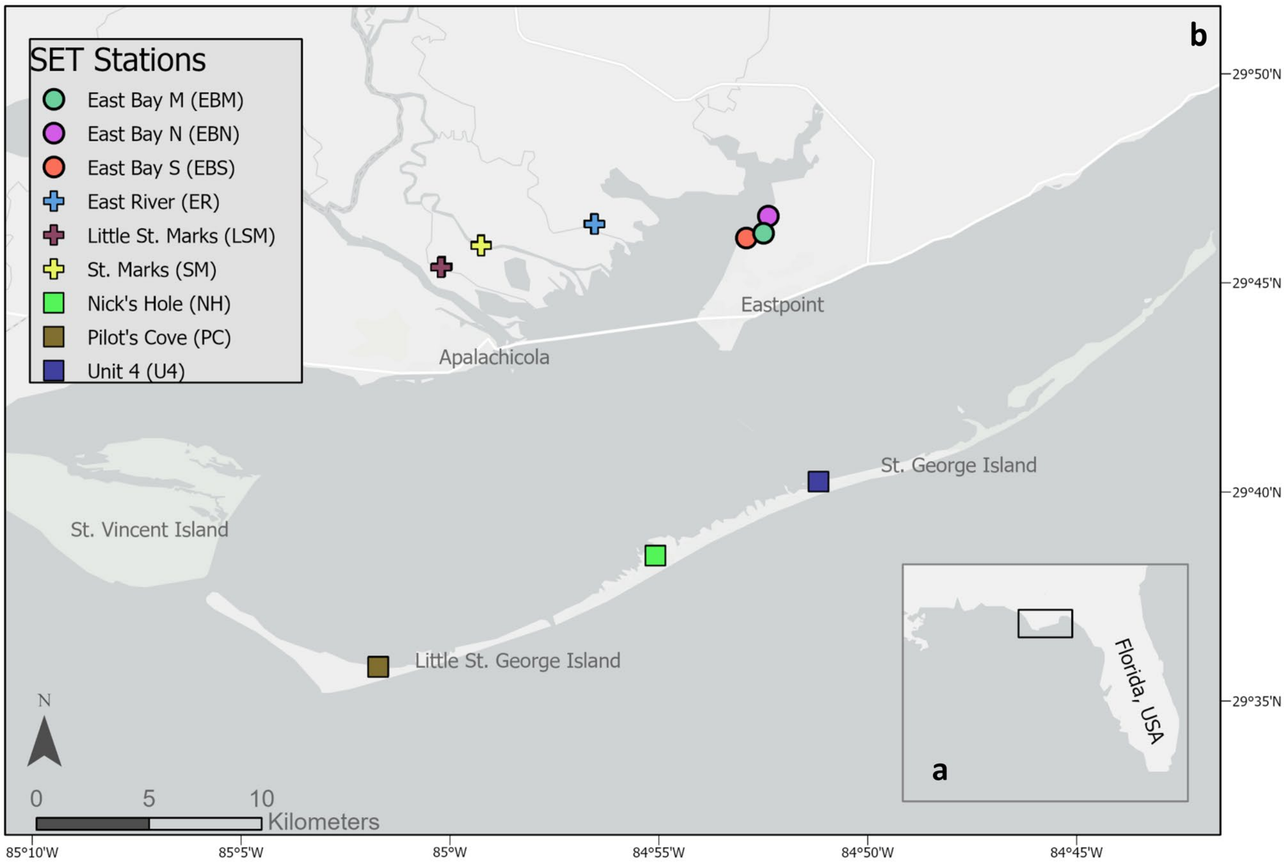

Fig. 1 Location of SET stations along the northern coast of Florida (panel a) and within the Apalachicola Bay complex (panel b). Sites denoted by a circle indicate stations at bayside sites, while crosses show stations at riverine sites and squares are stations on barrier islands. Color corresponds to station names. Two SETs are located at each station

downstream (Williams and Wolman 1984). Furthermore, the Apalachicola Bay estuary has been frequently affected by tropical storms and hurricanes (Edmiston 2008). Regional relative SLR has averaged 2.70 ± 0.61 mm year^{-1} between 1967 and 2021 ($RSLR_{historical}$; NOAA Tides and Currents, Station 8728690). In the last decade (2010–2021), the estuary has seen an acceleration to 11.46 ± 0.57 mm year^{-1} ($RSLR_{recent}$; NOAA Tides and Currents).

Two hurricanes affected the area within 60 km of the study sites between 2013 and 2020: Hurricanes Hermine (2016; Category 1) and Michael (2018, Category 5; NOAA Historical Hurricane Tracks). Hurricane Hermine passed east of the study site and provided less than 1 m of storm surge recorded at the same tide gauge, and less than 7.5 cm of rainfall (Berg 2016). Hurricane Michael passed west of the study site, providing 2.35 m of storm surge at the tide gauge in Apalachicola and 7.6–12.5 cm of rainfall, as well as causing an estimated $25 billion in damage to the area (Beven et al. 2019). As a result of the low impact of Hurricane Hermine on the sites used in this study, we exclusively considered the effect of Hurricane Michael on our study sites.

Coastal wetlands in three geomorphic settings were selected in the Apalachicola Bay National Estuarine Research Reserve for monitoring of surface elevation and accretion using rSET-MH methods. Riverine sites were located along the coastal edge of three distributaries of the Apalachicola River: East River (ER), St. Marks River (SM), and Little St. Marks River (LSM, Fig. 1). Each riverine site contained two SET stations: one located within a monoculture of *Cladium jamaicense* (sawgrass; LSM-J, SM-J, ER-K) and one located farther from the river's edge within *Taxodium distichum* (cypress; LSM-W; SM-B; ER-W). These sites receive freshwater inflow from the distributaries of the Apalachicola River, and surface water salinities range from 0 to 3 ppt (Edmiston 2008). Tidal fluctuations at these riverine sites are less than 0.15 m (Light et al. 1998).

Bayside sites were located along the coastal edge of East Bay, a 45 km^2 bay located north and east of the Apalachicola River delta with an average depth of 0.70 m (Edmiston 2008). East Bay receives freshwater inflow from both the Apalachicola River and its distributaries, as well as Tate's Hell Swamp. Salinities range between 3 and 6 ppt (Edmiston 2008) and marshes within these sites are dominated by *Juncus* *roemerianus* (black needlerush). The three bayside sites were East Bay S (EBS), East Bay N (EBN), and East Bay M (EBM; Fig. 1). Both SET stations at each bayside site were within 2 m of the shoreline edge, with both SET stations at each site equidistant from the shoreline.

The barrier island sites were located along the interior, back-barrier coastal margins of Little St. George Island (Pilot's Cove, PC) and St. George Island (Unit 4, U4; Nick's Hole, NH; Fig. 1). Vegetation at NH is predominantly *J. roemerianus*. Pilot's Cove and U4 vegetation is a mix of *J. roemerianus* and *Spartina alterniflora*, though U4 also contains encroaching red mangroves (*Rhizophora mangle*; Snyder et al. 2021; Steinmuller et al. 2022). At each of the barrier island sites, SET stations were originally constructed so that one station occupied low elevation marsh (*Spartina alterniflora)*, and the other occupied high elevation marsh (*Juncus roemerianus*).

Surface Elevation and Accretion

Each site contained two stations that each contained a rod-surface elevation table co-located with three feldspar marker horizons, deployed during 2011 and 2012 by the Apalachicola National Estuarine Research Reserve. Metal rods were driven until refusal and leveled relative to the US geodetic network (sensu Cahoon et al. 2002; Callaway et al. 2013; Lynch et al. 2015). Permanent boardwalk structures were installed around the SET-MH footprint to minimize disturbance of the measurement area. Surface elevation tables were measured with varying frequency, with a minimum of 2 measurements per year, spaced 6 months apart. During sampling, an extendable platform was deployed across the station to access the rod, upon which a SET arm consisting of a stainless steel coupler and arm fitted with 9 holes was attached (Cahoon et al. 2002). Using a compass and level, the SET arm was oriented to each cardinal direction and leveled. At each cardinal direction, fiberglass pins were placed into each of the 9 holes on the SET arm and lowered to the marsh surface. Pin heights were recorded to the nearest millimeter at each cardinal direction for a total of 36 individual measurements of surface elevation per SET station per sampling.

Measurements of accretion were conducted simultaneously with measurements of surface elevation. Feldspar was evenly spread within three 50 cm by 50 cm areas on the margins of the SET footprint. Initial MH plots were established during SET installation. During sampling, MH samples were taken via trowel from each of the three plots and a minimum of 1 observation (and a maximum of 4 observations) were made of the distance between the top of the feldspar layer and the soil surface (Lynch et al. 2015). Following measurement, samples were returned to plots and flagged to prevent re-sampling and to minimize disturbance to the plot. Feldspar horizons were re-deployed in a different area after the marker horizon could no longer be located.

Soil Sampling

During October 2021, soils adjacent to each SET station were sampled by pushcore (all barrier island sites, East Bay D, East Bay S) and/or Russian peat corer (all river sites, East Bay M, East Bay N) in triplicate. Different collection methods were used depending on substrate type, with obviously organic soils sampled by Russian peat corer and sandy sites sampled via pushcore. Soils sampled by pushcore were extruded into a single 15 cm interval, while soils sampled by the Russian peat corer were sectioned to keep the top 15 cm of soil. Both were transported back to the laboratory on ice. Field-moist soils were weighed and homogenized, and subsamples (approximately 20 g) were dried at 60 °C for 72 h or until a constant weight was achieved. The subsample dry weights were used to determine bulk density and subsequently homogenized using a mortar and pestle. Dried, ground subsamples were analyzed for percent organic matter (OM) via the loss-on-ignition method (Dean 1974), where subsamples were combusted for 3 h at 550 °C in a muffle furnace. Loss-on-ignition was calculated as the initial weight of the sample minus the weight of sample following combustion.

Statistical Analysis

Data analysis was performed in R (Version 4.1.0; R Institute for Statistical Computing, Vienna, Austria) with R Studio RStudio (Version 1.4.1717; RStudio Inc., Boston, MA, USA). Relative elevation (mm) for each individual pin at each sampling station at each time point was calculated as the observed pin height (mm) minus the initial pin height (mm). In order to compare elevations across geomorphic settings, relative elevation was used in the model rather than absolute elevation, which includes the orthoheight of the SETs. To test for differences in relative surface elevation change, a mixed-effect linear model (lme, package "nlme") was run, where fixed effects were elapsed years, geomorphic setting, and time period (pre- or post-Michael). Random effects included the effect of individual pins, nested within bearing/SET arm, which was nested within the individual SET stations.

Vertical accretion rates were calculated as the average height of the soil surface above the feldspar marker horizon during each sampling, divided by the elapsed time since the marker was placed (in years). If a feldspar horizon had been replaced since the initial horizon deployment, vertical accretion rates were calculated as the average height above the soil surface above the current feldspar marker horizon plus the last recorded average height of the previously deployed horizon, divided by the cumulative elapsed time of both horizons (i.e., Feher et al. 2020). These rates were calculated for each individual feldspar plot and then averaged at the SET station level. Because of difficulty associated with recovering feldspar at many of the stations, vertical accretion measurements lacked the temporal resolution required to test for differences associated with Hurricane Michael. A one-way ANOVA was used to identify differences in mean cumulative vertical accretion rates associated with geomorphic setting. No accretion was measured in the drowned SET stations (PC1, NH2).

Differences in soil physicochemical characteristics (bulk density, organic matter content) among geomorphic settings were determined via a one-way ANOVA. Pearson product-moment correlations were used to correlate soil physicochemical characteristics and vertical accretion rates.

Results

Differences Among Geomorphic Settings

Average cumulative accretion rates were significantly different between geomorphic settings ($p = 0.003$, F value = 9.505), with lower rates in the bayside sites, 5.16 ± 0.75 mm year^{-1}, compared to rates in riverine, 12.58 ± 1.24 mm year^{-1}, and barrier island sites, 10.47 ± 2.15 mm year^{-1}. Lowest station-level accretion rates averaged 2.76 ± 0.43 mm year^{-1}, observed at East Bay S (EBS-B), and greatest accretion rates averaged 16.87 ± 2.08 mm year^{-1} at Nick's Hole (NH1; Table 1, Fig. 2). Accretion rates were correlated to surface elevation change (across the entire timescale; $r = 0.478$).

Bulk density was different among geomorphic settings ($p < 0.001$), with barrier islands significantly different from bayside and riverine sites, which did not differ from each other. Bulk density increased from averages of 0.032 ± 0.003 g cm^{-3} and 0.053 ± 0.004 g cm^{-3} at the riverine and bayside sites, respectively, to an average of 0.420 ± 0.059 g cm^{-3} at barrier island sites. Organic matter content differed significantly between geomorphic settings ($p < 0.001$), with barrier islands containing the lowest % OM (5.59 ± 1.25%), followed by bayside (44.2 ± 2.86%) and riverine sites (52.5 ± 2.64%), which were not different from each other (Fig. 2). Organic matter content was negatively correlated to bulk density ($r = -0.90$). Within the riverine sites, there was a positive relationship between average accretion rates and OM content (r = 0.84; Fig. 3). Bayside sites showed significant negative relationships between average accretion rates and soil OM ($r = 0.84$) and average accretion rates and bulk density ($r = 0.74$, Fig. 3). Barrier island sites showed no significant relationship between either average accretion rates or soil OM (Fig. 3).

Response to Acute and Chronic Disturbance Among Geomorphic Settings

Rates of elevation change differed with the interaction between geomorphic setting and time period (pre- vs. post-Michael, p < 0.001; Fig. 4). During the pre-Michael period, there were no differences among geomorphic setting surface elevation change rates (Fig. 4). Between pre- and post-Michael time periods, barrier island surface elevation change rates did not differ (Fig. 4). At the bayside and riverine sites, the trajectory of surface elevation change steepened from pre- to post-Michael periods, with riverine surface elevation change rates being the highest (Fig. 4, Table 1). Rates of surface elevation change at individual SET stations ranged from −13.07 ± 0.74 mm year^{-1} at PC1 in the pre-Michael period to 17.21 ± 3.47 at LSM-J in the post-Michael period (Fig. 2, Table 1). Post-Michael rates of surface elevation change were positively correlated with average accretion rates (r = 0.73).

All bayside SET stations demonstrated an elevation deficit (both pre- and post-Michael) and an accretion deficit relative to the recent acceleration in $RSLR_{recent}$ (Table 1; Fig. 2). Bayside SET stations demonstrated higher accretion rates than $RSLR_{historical}$, and generally higher trends in surface elevation change post-Michael (Table 1; Fig. 2). Pre-Michael surface elevation change rates were greater than $RSLR_{historical}$ at 2 out of 6 SET stations (Fig. 2). With the exception of two stations, riverine SET stations demonstrated an accretion deficit compared to $RSLR_{recent}$ (Table 1; Fig. 2). Post-Michael trends in surface elevation were generally higher than either rate of RSLR, while pre-Michael surface elevations were lower than $RSLR_{recent}$ at all stations, and greater than $RSLR_{historical}$ at 2 out of 6 stations (Fig. 2). The drowned barrier island SETs (PC1 and NH2) showed extreme pre- and post-Michael surface elevation deficits relative to both RSLR rates (Fig. 2). Accretion at these drowned barrier island sites could not be quantified. The remaining barrier island SET stations demonstrated surface elevation change rates greater than or equal to $RSLR_{historical}$ both pre- and post-Michael (Fig. 2). All surface elevation change rates were lower than $RSLR_{recent}$. Nick's Hole 1 displayed a higher rate of accretion than either RSLR rate, however was the only barrier island station to demonstrate such a trend (Fig. 2).

Table 1 Linear trends of relative elevation (mm) regressed against elapsed time to determine surface elevation change trends (mm $year^{-1}$) for each SET station, nested within geomorphic setting, for both pre- and post-Michael time periods. df denotes degrees of freedom

		Pre-Michael					*Post-Michael*						
Geomorphic setting	**SET station**	**df**	***F* statistic**	**Surface elevation trend (mm $year^{-1}$)**	**Standard error**	***p* value**	**df**	***F* statistic**	**Surface elevation trend (mm $year^{-1}$)**	**Standard error**	***p* value**	**Average accretion rate (mm $year^{-1}$)**	**Standard error**
	EBS-B	538	20.1	1.21	0.27	< 0.0001	178	25.4	−7.36	1.46	< 0.0001	2.76	0.43
	EBS-C	574	0.5	0.2	0.28	0.474	142	30.4	8.49	1.54	< 0.0001	4.03	0.65
Bayside	EBM-D	538	141.3	3.68	0.31	< 0.0001	106	7.4	8.27	3.04	0.008	7.69	0.78
	EBM-E	538	313.7	5.56	0.31	< 0.0001	106	1.8	3.32	2.47	0.182	6.77	1.3
	EBN-F	538	103	2.79	0.27	< 0.0001	142	21.9	8.47	1.81	< 0.0001	4.34	0.73
	EBN-G	538	8.9	0.84	0.29	0.003	141	8.3	4.22	1.47	0.005	5.34	0.65
	SM-B	502	86.2	3.59	0.39	< 0.0001	142	37.1	12.24	2.01	< 0.0001	14.49	3.09
	LSM-J	502	249.1	5.36	0.34	< 0.0001	138	24.6	17.21	3.47	< 0.0001	15.54	3.65
Riverine	SM-J	430	79.1	4.73	0.53	< 0.0001	141	11.6	9.32	2.74	0.0009	11.79	3.48
	ER-W	502	28.2	1.99	0.37	< 0.0001	142	24.3	12	2.44	< 0.0001	8.53	2.84
	ER-K	502	183.1	6.86	0.51	< 0.0001	142	14.3	9.03	2.39	0.0002	9.68	1.7
	LSM-W	538	19.8	1.82	0.41	< 0.0001	141	54.1	13.8	1.88	< 0.0001	15.41	3.17
	NH1	466	63.1	2.67	0.34	< 0.0001	177	55.1	11.15	1.5	< 0.0001	16.87	2.08
	NH2	430	1.9	−0.57	0.41	0.166	142	36.7	−9.17	1.51	< 0.0001	-	-
Barrier island	PC1	466	308	−13.07	0.74	< 0.0001	142	0.6	−4.09	5.07	0.422	-	-
	PC2	466	487.3	10.77	0.49	< 0.0001	142	0.8	2.79	3.18	0.373	8.59	2.32
	U41	466	115.2	4.8	0.45	< 0.0001	178	13.4	6.68	1.83	0.0003	8.9	1.44
	U42	429	39.3	−2.18	0.35	< 0.0001	178	15.8	5.73	1.44	0.0001	7.52	1.08

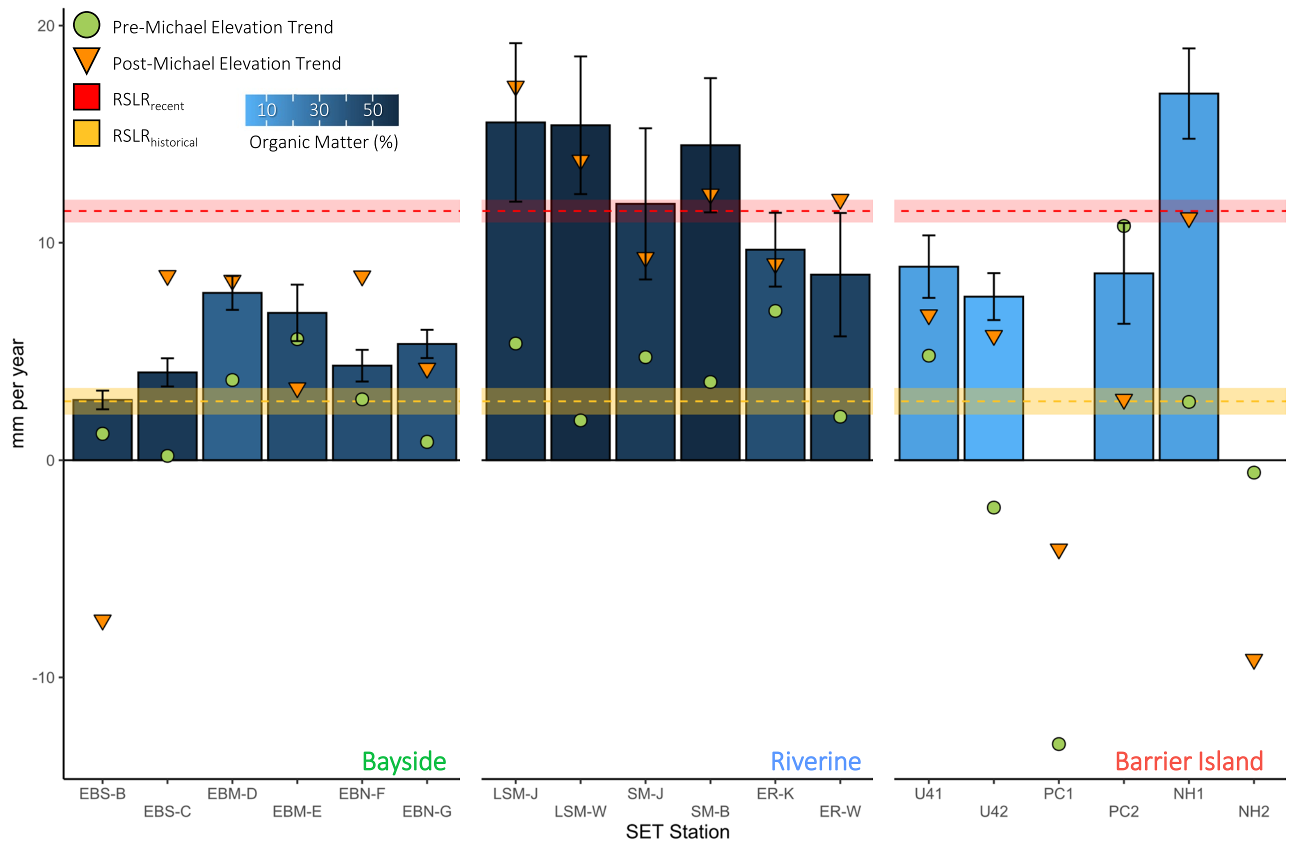

Fig. 2 Average accretion rates (mm year^{-1}; bars) colored by organic matter content (%) at each SET station, grouped by geomorphic setting. Error on bars is ± standard error. Points indicate rates of surface elevation change (mm year^{-1}) at each SET station pre-Michael (green circles) and post-Michael (orange triangles). Horizontal dotted lines indicate calculated $RSLR_{recent}$ (red; 11.46 ± 0.57 mm year^{-1}) and $RSLR_{historical}$ (yellow; 2.70 ± 0.61 mm year^{-1}). Associated shaded area denotes standard error on RSLR rates. No accretion rates were quantifiable for drowned SET stations (PC1 and NH2)

Discussion

Surface elevation change rates (across the entire timescale) at all SET stations in all geomorphic settings were roughly 25% lower than accretion rates, indicating that shallow subsidence is offsetting increases in marsh elevation due to accretion. Shallow subsidence is defined in the SET literature as subsidence occurring within the soil profile above the terminus of the SET rod and in this case can be attributed to subsurface compaction (Cahoon et al. 1995; Cahoon et al. 2006; Cahoon et al. 2020). In a survey of 11 tidal marshes across the USA, Raposa et al. (2016) reported a similar trend of accretion rates exceeding rates of surface elevation change in 45% of sites. Similarly, studies spanning the Delaware Estuary, Barnegat Bay, NJ (Haaf et al. 2022), five National Wildlife Refuges along the Texas coast (Moon et al. 2022), and 9 sites along the Mississippi River in Louisiana (Lane et al. 2006) have reported accretion rates exceeding rates of surface elevation change in the majority (if not all) studied SET-MH stations. This general trend, across broad geographic regions and in Apalachicola Bay, suggests that surface accretion rates are not good proxies of surface elevation change; using surface accretion rates as a proxy for elevation would overestimate the resilience of these sites to relative SLR (Raposa et al. 2016). However, in the case of a storm event providing a sediment and/or wrack subsidy, surface elevation change rates can increase to equal (or exceed) accretion rates (i.e., all riverine stations, 3 of 6 bayside stations) for some geomorphic settings. Though it is unclear over what timescale these high rates of surface elevation change will persist, this observed trend demonstrates the importance of sediment and/or wrack input on maintaining vertical position within the tidal frame for some geomorphic settings.

Influence of Geomorphic Setting on Surface Elevation Trends

The relationship between high accretion rates and low rates of surface elevation change in this study agree with previous

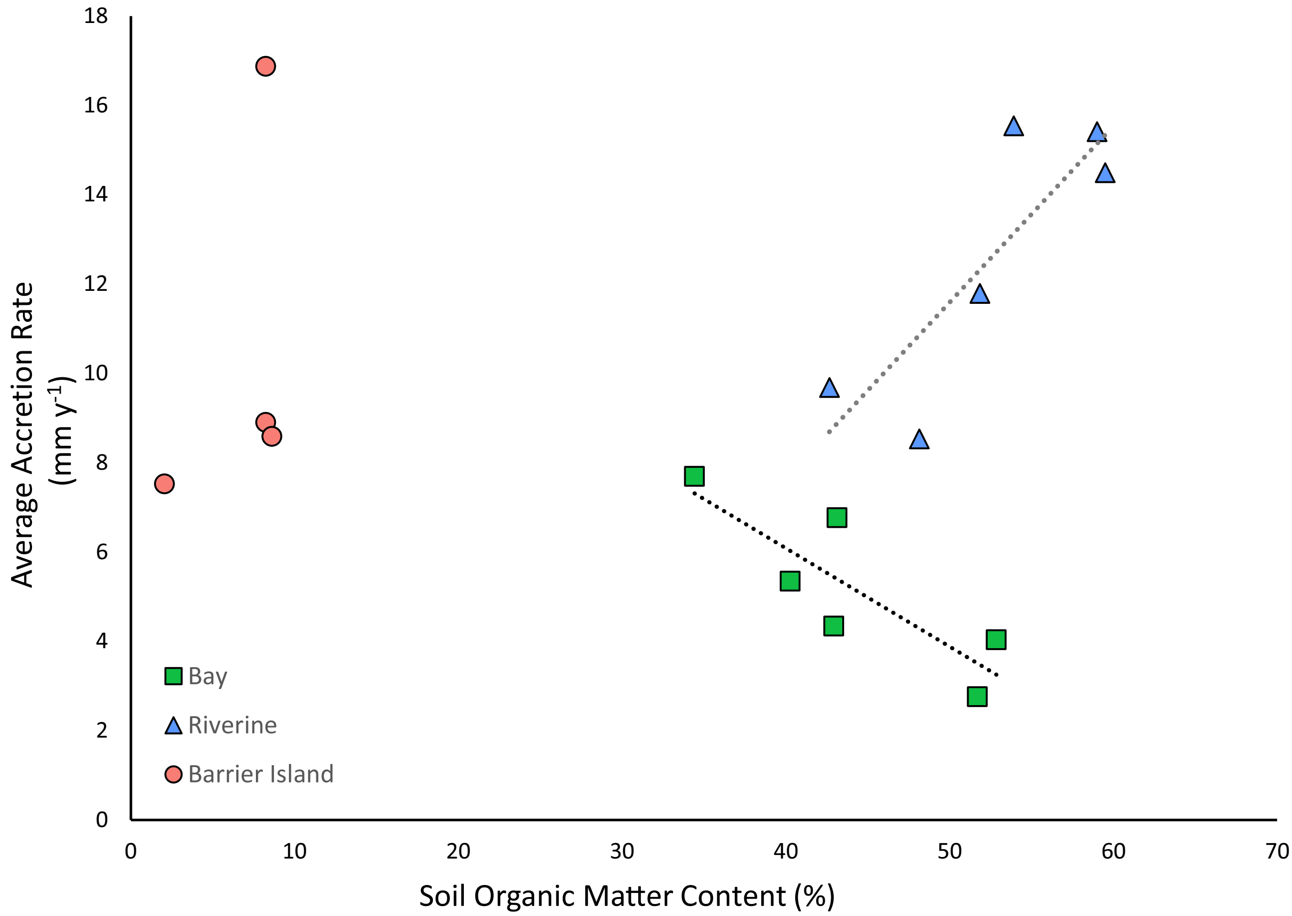

Fig. 3 Linear relationships between average accretion rates (mm year^{-1}) and soil organic matter content (%) at riverine, bay, and barrier islands, where each point represents an individual SET station. $R^2 = 0.71$ for both trendlines (riverine and bay)

observations from Gulf of Mexico coastal marshes (Cahoon et al. 2006), though both rate types are greater here than those reported elsewhere in the northern Gulf of Mexico. The lower accretion and elevation change rates (3 mm year^{-1} and 2.5 mm year^{-1}, respectively) reported by Cahoon et al. (2006) for sites comparable to our bayside sites are lower than average accretion and elevation change rates reported for our bayside sites, likely attributable to site-level differences in sediment supply. In comparing our barrier island rates of accretion and elevation to Cahoon et al. (2006), we see much greater accretion and much smaller elevation change at our sites, which is partly explained by our inclusion of drowned SETs and relatively high sediment supply and/or redistribution at our sites.

Dominant vegetation type plays an important role in the dynamics that shape geomorphic settings (Fagherazzi et al. 2004). Numerous studies have demonstrated the effects of vegetation type on surface elevation within coastal wetlands (Cahoon et al. 2000; Rooth and Stevenson 2000; Boumans et al. 2002; Rogers et al. 2005; Wallace et al. 2005; Rogers et al. 2006; Ibáñez et al. 1999; Lovelock et al. 2011), and we observed some variability between vegetation types at our riverine sites, with sawgrass stations (LSM-J; SM-J; ER-K) demonstrating higher rates of elevation gain than cypress-dominated stations (LSM-W; SM-B; ER-W. However, sawgrass-dominated stations occupied lower relative elevations and were located closer to the distributary river channels than cypress-dominated sites. The co-incidence of these variables does not allow for distinguishing whether elevation gains are attributable to differences between autochthonous production within vegetation types, sediment trapping efficiencies of marsh versus swamp (Morris et al. 2002), relative proximity to freshwater inputs, relative elevation, or some combination thereof. Freshwater inputs can facilitate the deposition of sediment (evidenced through the comparatively lower OM content within sawgrass than cypress sites) preferentially at lower relative elevations or in areas with high sediment trapping efficiencies, flush soil pore spaces to remove soil anaerobiosis, and deliver nutrients to stimulate primary productivity (Cahoon et al. 2006).

Geomorphic setting and soil physicochemistry are fundamentally linked (Jackson et al. 2014), and our results

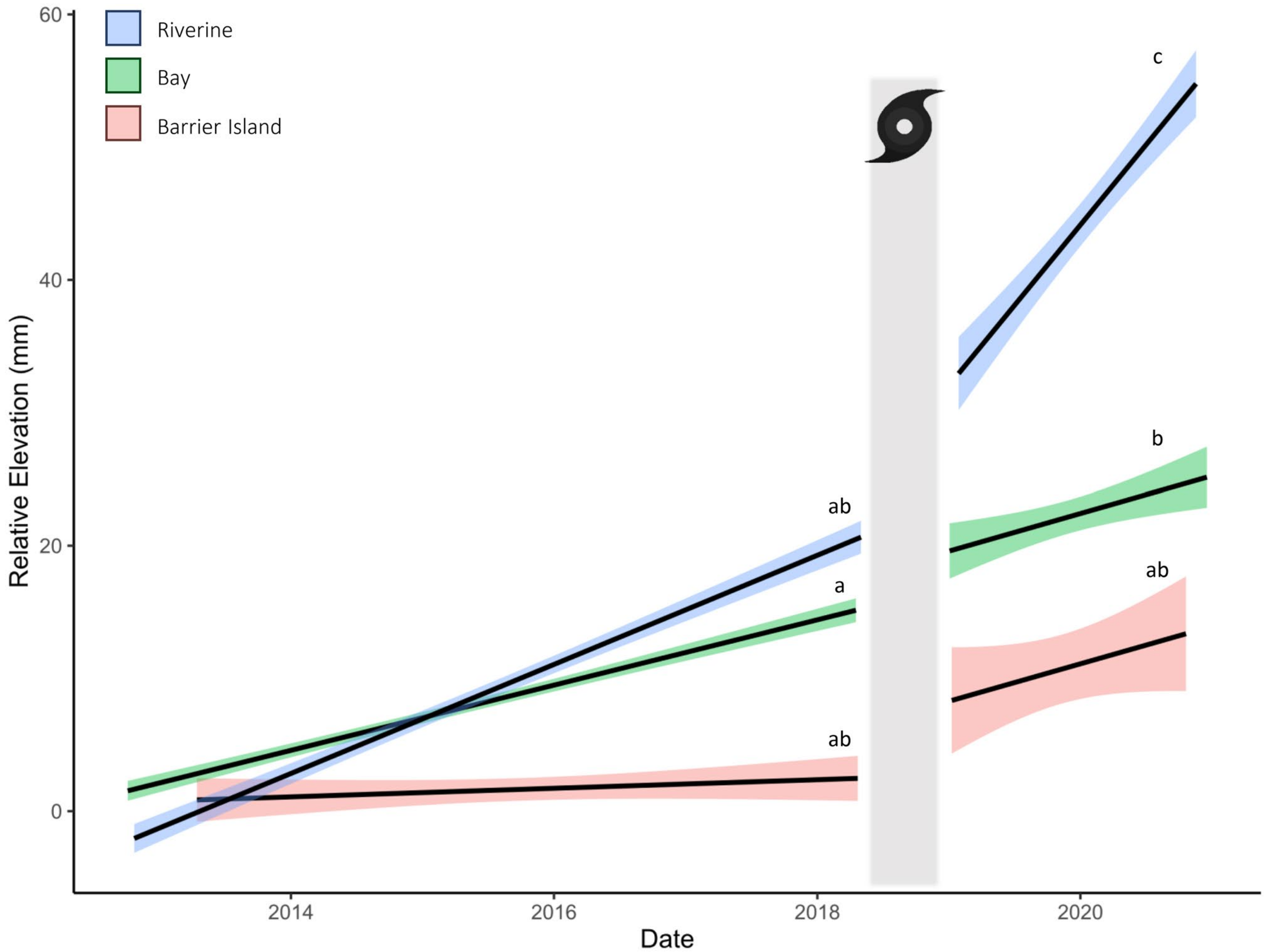

Fig. 4 Average relative surface elevation trends regressed with date for each geomorphic setting, as denoted by color, for pre- and post-Hurricane Michael periods. Shaded area around lines illustrates standard error of conditional means. Gray shaded area denotes break in available data associated with Hurricane Michael. Lowercase letters denote significant differences among rates

indicated differences in the relationship between soil physicochemical parameters and vertical change between geomorphic settings. Accretion at the riverine sites demonstrated a positive relationship with soil OM content, in concordance with previous research that has suggested soil OM is a limiting factor controlling accretion within coastal mangrove and marshes (Morris et al. 2016; Breithaupt et al. 2017). It is not possible from the data at hand to determine whether this OM is derived from autochthonous (root production, litter deposition) or allochthonous inputs (organic inputs from riverine sources). Interestingly, bayside sites demonstrated the opposite trend, as the rate of accretion decreased with increasing soil OM content and bulk density. The volume, and thus the packing density, of OM structures in soil can vary widely (Morris et al. 2016; Breithaupt et al. 2017); at the bayside sites, organic material is more tightly packed than at the riverine sites, which contributes to the two geomorphic settings having similar OM contents, but opposite relationships between soil OM and accretion rates.

Response to Acute Disturbance: Hurricane Michael

Hurricane Michael impacted all sites in October of 2018 with an estimated maximum 29.5 cm of rainfall (Beven et al. 2019) and up to 4.74 m of storm surge (Wang et al. 2020; J. Garwood, personal observation). With the exception of one bayside site (EBS-C), all SETs showed an increase in surface elevation immediately following landfall of Hurricane Michael (Supplemental Fig. 1, Table 1). Sediment and/or wrack deposition could explain the increase in surface elevation trends observed at the riverine and bayside sites (Cahoon et al. 2003; Cahoon et al. 2006; McKee and Cherry 2009; Whelan et al. 2009; Rogers et al. 2013; Moon et al. 2022). High energy storms mobilize marine sediments, which are then deposited via storm surge on the wetland soil surface (Whelan et al. 2009; Castañeda-Moya et al. 2010; Smoak et al. 2013; Breithaupt et al. 2019; Breithaupt et al. 2020). The addition of storm-mobilized sediment subsidizes short-term vertical accretion, resulting in a net elevation gain (Cahoon 2006; Smoak et al. 2013; Feher et al. 2020). Storms can also resuspend and redistribute local sediments (Perez et al. 2000). Similarly, storm-deposited wrack can increase soil elevation temporarily (Cahoon et al. 2006). In the long term, wrack can either further promote elevation gains by providing nutrient subsidies to stimulate primary production or further decrease elevation through stimulation of heterotrophic mineralization of organic material (Kuzyakov 2010).

After Hurricane Michael, two bayside stations (EBM-E and EBM-D) demonstrated short-term elevation gains that were eventually followed by elevation losses (Supplemental Fig. 1). Studies have demonstrated that increases in elevation following extreme weather events are often temporary, with soil elevation subsequently decreasing by compaction under the weight of mineral additions or through post-storm decomposition of organic components (Cahoon et al. 2006 and references therein; Moon et al. 2022). The impacts of storm events have been shown to persist for decades in some cases (Feher et al. 2020; Cahoon et al. 2011), but Hurricane Michael occurred toward the end of our 8-year elevation record. While many of our sites demonstrated storm-related elevation gains, further monitoring sites is necessary to determine whether these elevation gains represent a temporary or long-term trend.

Response to Chronic Disturbance: Vulnerability to Sea-Level Rise

The average rate of relative SLR at Apalachicola between 1967 and 2021 was 2.70 ± 0.61 mm year^{-1} (NOAA Tides and Currents, Station 8728690). However, in the decadal time period of our observations (between 2010 and 2021), RSLR at Apalachicola was 11.46 ± 0.57 mm year^{-1}. Compared to the contemporaneous rate of RSLR, all sites across all geomorphic settings in this study displayed elevation gain deficits prior to Hurricane Michael (Fig. 2). Accretion at bayside sites was the lowest of any geomorphic setting in this study, likely a facet of a decreased or insubstantial sediment supply. The combination of elevation and accretion deficits suggests that bayside sites are the most vulnerable geomorphic setting to RSLR in this region. Timelines estimated using coupled hydrodynamic (ADCIRC) and marsh equilibrium model (Hydro-MEM) simulations anticipate submergence of these sites within 50 years

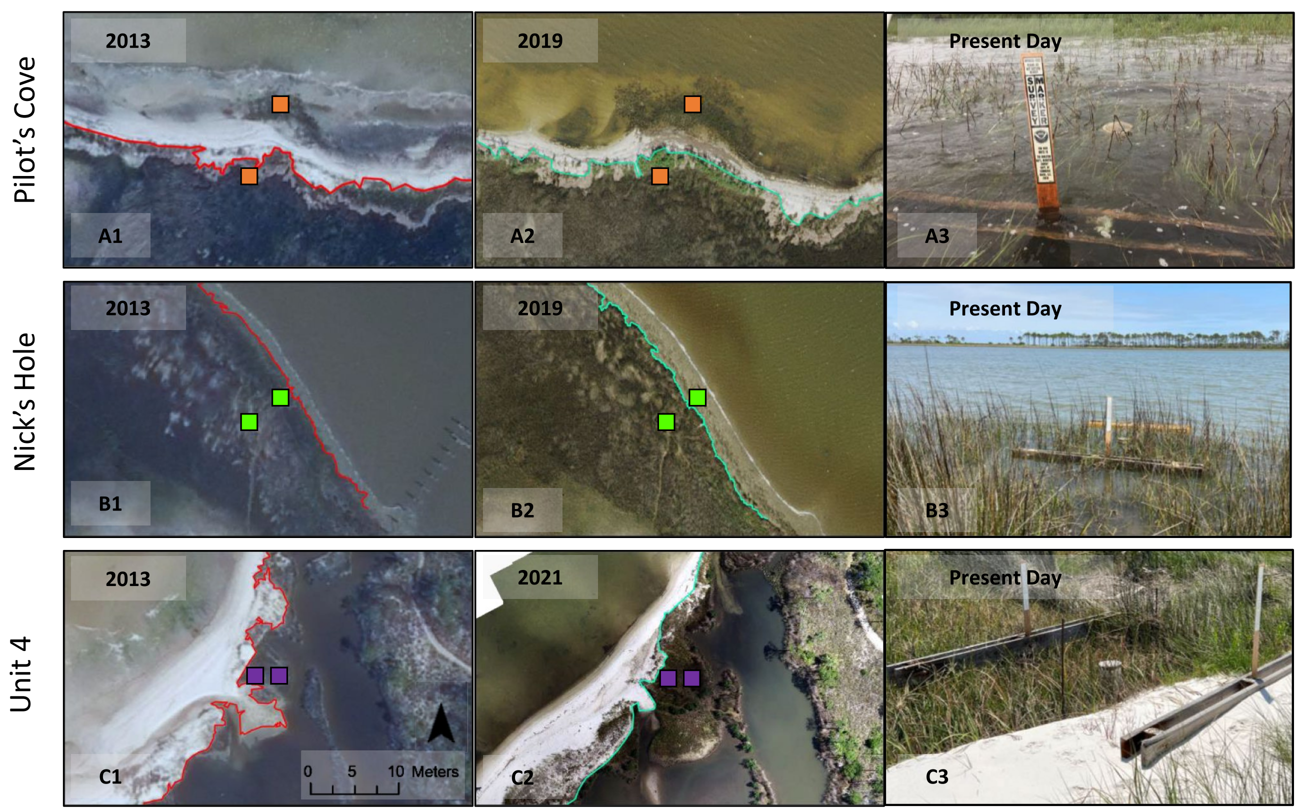

Fig. 5 Aerial imagery from each of the barrier island sites (Pilot's Cove, Nick's Hole, and Unit 4) depicting the location of the SET stations (depicted by squares) relative to the shoreline immediately following station installation in 2013 (A1, B1, C1), in the most recently available imagery (A2 2019, B2 2019, C2 2021) and current photos of the seaward-neighboring SET station at each site (A3, B3, C3). Pilot's Cove and Nick's Hole have drowned SET stations, and Unit 4 is occupied by a transgressing sand berm

(Alizad et al. 2016). In contrast, riverine sites are less vulnerable to $RSLR_{recent}$, demonstrated by high accretion rates and high rates of surface elevation change post-Michael. If pre-Michael surface elevation increases are the norm for riverine sites, and recent post-Michael rates are just a short-term exception, then riverine sites are more vulnerable to recent rates of RSLR. Alizad et al. (2016) estimated submergence of these sites within a similar timescale as bayside sites.

In addition to the vertical threat of RSLR, barrier island SET stations are also vulnerable to lateral erosion due to their location near the interior shoreline of the barrier islands. Two SET stations drowned over the course of the study, and a third that has since been inundated by overwash deposits of sand that seem likely to precede imminent erosion in the near future (Fig. 5). This vulnerability to lateral shoreline movement was not identified in the SET-MH data until submergence occurred. Over the course of this study (2013–2020), substantial lateral erosion occurred at each barrier island site (Fig. 5), representing shoreline loss on the order of meters. This component of lateral erosion is missing from estimates of submergence timelines and highlights the limitations of reliance on a single method for quantifying wetland vulnerability. The submergence of two SET stations, and the vulnerability of others via shoreline erosion, calls attention to the importance of coupling SET-MH measurements with measures of horizontal change to form a more accurate prediction of the vulnerability of these sites to relative SLR.

Supplementary Information The online version contains supplementary material available at https://doi.org/10.1007/s12237-022-01131-4.

Funding Funding for HES was provided by a post-doctoral fellowship for the Coastal and Marine Laboratory supported by the Office of the Vice President for Research at Florida State University. JLB and KME were supported by Triumph Gulf Coast Inc. Project #69: Apalachicola Bay System Initiative. The authors wish to thank Sydney Rodetsky, Kindle Hon, and Alek Valles for laboratory and field assistance. Access to research sites and data was provided by the Apalachicola National Estuarine Research Reserve. Thanks to the National Oceanic Atmospheric Administration, National Estuarine Research Reserve System for their generous support with funding (grant numbers NA14NOS4200041 and NA15NOS4200102) and the Florida Department of Environment protection for their support of Reserve staff and equipment.

Declarations

Competing Interests The authors declare no competing interests.

References

Adame, M.F., D. Neil, S.F. Wright, and C.E. Lovelock. 2010. Sedimentation within and among mangrove forests along a gradient of geomorphological settings. *Estuarine, Coastal and Shelf Science* 86 (1): 21–30.

Alizad, K., S.C. Hagen, J.T. Morris, S.C. Medeiros, M.V. Bilskie, and J.F. Weishampel. 2016. Coastal wetland response to sea-level rise in a fluvial estuarine system. *Earth's Future* 4 (11): 483–497.

Baustian, J.J., and I.A. Mendelssohn. 2015. Hurricane-induced sedimentation improves marsh resilience and vegetation vigor under high rates of relative sea level rise. *Wetlands* 35: 795–802. https://doi.org/10.1007/s13157-015-0670-2.

Berg, R. 2016. National Hurricane Center Tropical Cyclone Report-Hurricane Hermine. National Hurricane Center, National Oceanic and Atmospheric Administration, National Weather Service, Miami, FL, Rep. AL092016.

Beven, J.L., R. Berg, and A. Hagen. 2019. *National hurricane center tropical cyclone report: Hurricane Michael*. Miami, FL: US National Oceanic and Atmospheric Administration (NOAA), National Hurricane Center.

Boumans, R.M., M. Ceroni, D.M. Burdick, D.R. Cahoon, and C.W. Swarth. 2002. *Sediment elevation dynamics in tidal marshes: functional assessment of accretionary biofilters*. Durham, NH: NOAA/UNH Cooperative Institute for Coastal and Estuarine Environmental Technology (CICEET) Final technical Report.

Breithaupt, J.L., N. Hurst, H.E. Steinmuller, E. Duga, J.M. Smoak, J.S. Kominoski, and L.G. Chambers. 2019. Comparing the biogeochemistry of storm surge sediments and pre-storm soils in coastal wetlands: Hurricane Irma and the Florida Everglades. *Estuaries and Coasts*. https://doi.org/10.1007/s12237-019-00607-0.

Breithaupt, J.L., J.M. Smoak, R.H. Byrne, M.N. Waters, R.P. Moyer, and C.J. Sanders. 2018. Avoiding timescale bias in assessments of coastal wetland vertical change. *Limnology and Oceanography* 63 (S1): S477–S495. https://doi.org/10.1002/LNO.10783.

Breithaupt, J.L., J.M. Smoak, T.S. Bianchi, D.R. Vaughn, C.J. Sanders, K.R. Radabaugh, M.J. Osland, L.C. Feher, J.C. Lynch, and D.R. Cahoon. 2020. Increasing rates of carbon burial in southwest Florida coastal wetlands. *Journal of Geophysical Research: Biogeosciences* 125 (2): e2019JG005349.

Breithaupt, J.L., J.M. Smoak, V.H. Rivera-Monroy, E. Castañeda-Moya, R.P. Moyer, M. Simard, and C.J. Sanders. 2017. Partitioning the relative contributions of organic matter and mineral sediment to accretion rates in carbonate platform mangrove soils. *Marine Geology* 390: 170–180.

Brinson, M.M. 1993. *A hydrogeomorphic classification for wetlands*. US: Environmental Laboratory.

Cahoon, D.R. 2006. A review of major storm impacts on coastal wetland elevations. *Estuaries and Coasts* 29 (6): 889–898. https://doi.org/10.1007/BF02798648.

Cahoon, D.R., B.C. Perez, B.D. Segura, and J.C. Lynch. 2011. Elevation trends and shrink-swell response of wetland soils to flooding and drying. *Estuarine, Coastal and Shelf Science* 91: 463–474.

Cahoon, D.R., D.J. Reed, and J.W. Day. 1995. Estimating shallow subsidence in microtidal salt marshes of the southeastern United States: Kaye and Barghoorn revisited. *Marine Geology* 128 (1–2): 1–9. https://doi.org/10.1016/0025-3227(95)00087-F.

Cahoon, D.R., D.J. Reed, J.W. Day, J.C. Lynch, A. Swales, and R.R. Lane. 2020. Applications and utility of the surface elevation table–marker horizon method for measuring wetland elevation and shallow soil subsidence-expansion. *Geo-Marine Letters* 40 (5): 809–815.

Callaway, J.C., D.R. Cahoon, and J.C. Lynch. 2013. The surface elevation table–marker horizon method for measuring wetland accretion and elevation dynamics. *Methods in Biogeochemistry of Wetlands* 10: 901–917.

Cahoon, D.R., J.R. French, T. Spencer, D. Reed, and I. Möller. 2000. Vertical accretion versus elevational adjustment in UK saltmarshes: An evaluation of alternative methodologies. *Geological Society, London, Special Publications* 175 (1): 223–238.

Cahoon, D.R., J.C. Lynch, B.C. Perez, B. Segura, R.D. Holland, C. Stelly, G. Stephenson, and P. Hensel. 2002. High-precision measurements of wetland sediment elevation: II. The rod surface elevation table. *Journal of Sedimentary Research* 72 (5): 734–739.

Cahoon, D.R., P. Hensel, J. Rybczyk, K.L. McKee, C.E. Proffitt, and B.C. Perez. 2003. Mass tree mortality leads to mangrove peat collapse at Bay Islands, Honduras after Hurricane Mitch. *Journal of Ecology* 91 (6): 1093–1105. https://doi.org/10.1046/j.1365-2745.2003.00841.x.

Cahoon, D.R., P.F. Hensel, T. Spencer, D.J. Reed, K.L. McKee, and N. Saintilan. 2006. Coastal wetland vulnerability to relative sea-level rise: wetland elevation trends and process controls. In *Wetlands and natural resource management*, 271–292. Springer.

Castañeda-Moya, E., R.R. Twilley, V.H. Rivera-Monroy, K. Zhang, S.E. Davis, and M. Ross. 2010. Sediment and nutrient deposition associated with Hurricane Wilma in mangroves of the Florida Coastal Everglades. *Estuaries and Coasts* 33 (1): 45–58.

Church, J.A., and N.J. White. 2006. A 20th century acceleration in global sea-level rise. *Geophysical Research Letters* 33 (1): L01602.

Dangendorf, S., C. Hay, F.M. Calafat, M. Marcos, C.G. Piecuch, K. Berk, and J. Jensen. 2019. Persistent acceleration in global sea-level rise since the 1960s. *Nature Climate Change* 9 (9): 705–710.

Danielson, T.M., V.H. Rivera-Monroy, E. Castañeda-Moya, H. Briceño, R. Travieso, B.D. Marx, E. Gaiser, and L.M. Farfán. 2017. Assessment of Everglades mangrove forest resilience: Implications for above-ground net primary productivity and carbon dynamics. *Forest Ecology and Management* 404: 115–125.

Darst, M.R., and H.M. Light. 2008. *Drier forest composition associated with hydrologic change in the Apalachicola River floodplain, Florida*. Prepared in cooperation with the Florida Department of Environmental Protection Northwest Florida Water Management District Scientific Investigations Report 2008–5062. http://www.usgs.gov/pubprod. Accessed May 2022.

Dean, W.E. 1974. Determination of carbonate and organic matter in calcareous sediments and sedimentary rocks by loss on ignition; comparison with other methods. *Journal of Sedimentary Research* 44 (1): 242–248.

Dürr, H.H., G.G. Laruelle, C.M. van Kempen, C.P. Slomp, M. Meybeck, and H. Middelkoop. 2011. Worldwide typology of nearshore coastal systems: Defining the estuarine filter of river inputs to the oceans. *Estuaries and Coasts* 34 (3): 441–458.

Edmiston, H.L. 2008. Apalachicola National Estuarine Research. *Reserve, a river meets the bay 50*.

Fagherazzi, S., M. Marani, and L.K. Blum. 2004. *The ecogeomorphology of tidal marshes*. American Geophysical Union.

Feher, L.C., M.J. Osland, G.H. Anderson, W.C. Vervaeke, K.W. Krauss, K.R.T. Whelan, K.M. Balentine, G. Tiling-Range, T.J. Smith, and D.R. Cahoon. 2020. The long-term effects of hurricanes Wilma and Irma on soil elevation change in Everglades mangrove forests. *Ecosystems* 23 (5): 917–931.

Haaf, L.A., E.B. Watson, T. Elsey-Quirk, K. Raper, A. Padeletti, M. Maxwell-Doyle, D. Kreeger, and D.J. Velinsky. 2022. Sediment accumulation, elevation change, and the vulnerability of tidal marshes in the Delaware Estuary and Barnegat Bay to accelerated sea level rise. *Estuaries and Coasts* 45 (2): 413–427. https://doi.org/10.1007/S12237-021-00972-9.

Ibañez, C., J.W. Day Jr., and D. Pont. 1999. Primary production and decomposition of wetlands of the Rhone Delta, France: interactive impacts of human modifications and relative sea level rise. *Journal of Coastal Research* 15: 717–731.

Jackson, R., J. Thompson, and R. Kolka. 2014. Wetland soils, hydrology, and geomorphology. University of California Press.

Kaye, C.A., and E.S. Barghoorn. 1964. Late quaternary sea-level change and crustal rise at Boston, Massachusetts, with notes on the autocompaction of peat. *Bulletin of the Geological Society of America* 75 (2): 63–80.

Kirwan, M.L., and J.P. Megonigal. 2013. Tidal wetland stability in the face of human impacts and sea-level rise. *Nature* 504 (7478): 53–60. https://doi.org/10.1038/nature12856.

Kuzyakov, Y. 2010. Priming effects: Interactions between living and dead organic matter. *Soil Biology and Biochemistry* 42 (9): 1363–1371.

Lane, R.R., J.W. Day Jr., and J.N. Day. 2006. Wetland surface elevation, vertical accretion, and subsidence at three Louisiana estuaries receiving diverted Mississippi River water. *Wetlands* 26 (4): 1130–1142.

Light, H.M., M.R. Darst, and J.W. Grubbs. 1998. *Aquatic habitats in relation to river flow in the Apalachicola River floodplain, Florida*. USGPO; US Geological Survey.

Lovelock, C.E., V. Bennion, A. Grinham, and D.R. Cahoon. 2011. The role of surface and subsurface processes in keeping pace with sea level rise in intertidal wetlands of Moreton Bay, Queensland. *Australia. Ecosystems* 14 (5): 745–757.

Lugo, A.E., and S.C. Snedaker. 1974. The ecology of mangroves. *Annual Review of Ecology and Systematics* 5 (1): 39–64. https://doi.org/10.1146/annurev.es.05.110174.000351.

Lynch, J.C., P. Hensel, and D.R. Cahoon. 2015. *The surface elevation table and marker horizon technique: a protocol for monitoring wetland elevation dynamics*. National Park Service.

McKee, K.L., D.R. Cahoon, and I.C. Feller. 2007. Caribbean mangroves adjust to rising sea level through biotic controls on change in soil elevation. *Global Ecology and Biogeography* 16 (5): 545–556. https://doi.org/10.1111/j.1466-8238.2007.00317.x.

McKee, K.L., and J.A. Cherry. 2009. Hurricane Katrina sediment slowed elevation loss in subsiding brackish marshes of the Mississippi River delta. *Wetlands* 29 (1): 2–15.

Moon, J.A., L.C. Feher, T.C. Lane, W.C. Vervaeke, M.J. Osland, D.M. Head, B.C. Chivoiu, D.R. Stewart, D.J. Johnson, J.B. Grace, K.L. Metzger, and N.M. Rankin. 2022. Surface elevation change dynamics in coastal marshes along the Northwestern Gulf of Mexico: Anticipating effects of rising sea-level and intensifying hurricanes. *Wetlands* 1: 3. https://doi.org/10.1007/s13157-022-01565-3.

Morris, J.T., D.C. Barber, J.C. Callaway, R. Chambers, S.C. Hagen, C.S. Hopkinson, B.J. Johnson, P. Megonigal, S.C. Neubauer, and T. Troxler. 2016. Contributions of organic and inorganic matter to sediment volume and accretion in tidal wetlands at steady state. *Earth's Future* 4 (4): 110–121.

Morris, J.T., P.V. Sundareshwar, C.T. Nietch, B. Kjerfve, and D.R. Cahoon. 2002. Responses of coastal wetlands to rising sea level. *Ecology* 83 (10): 2869–2877. https://doi.org/10.1890/0012-9658(2002)083[2869:ROCWTR]2.0.CO;2.

Mossa, J., et al. 2017. Anthropogenic landforms and sediments from dredging and disposing sand along the Apalachicola River and its floodplain. *Geomorphology* 294: 119–134.

Nuttle, W.K., H.F. Hemond, and K.D. Stolzenbach. 1990. Mechanisms of water storage in salt marsh sediments: The importance of dilation. *Hydrological Processes* 4 (1): 1–13.

Osland, M. J., et al. 2017. Assessing coastal wetland vulnerability to sea-level rise along the northern Gulf of Mexico coast: Gaps and opportunities for developing a coordinated regional sampling network. *PloS One* 12(9): e0183431.

Osland, M.J., L.C. Feher, G.H. Anderson, W.C. Vervaeke, K.W. Krauss, K.R.T. Whelan, K.M. Balentine, G. Tiling-Range, T.J. Smith, and D.R. Cahoon. 2020. A tropical cyclone-induced ecological regime shift: Mangrove forest conversion to mudflat in Everglades National Park (Florida, USA). *Wetlands* 40 (5): 1445–1458.

Paerl, H.W., J.D. Bales, L.W. Ausley, C.P. Buzzelli, L.B. Crowder, L.A. Eby, J.M. Fear, M. Go, B.L. Peierls, and T.L. Richardson. 2001. Ecosystem impacts of three sequential hurricanes (Dennis, Floyd, and Irene) on the United States' largest lagoonal estuary, Pamlico

Sound, NC. *Proceedings of the National Academy of Sciences* 98 (10): 5655–5660.
Perez, B.C., J.W. Day Jr., L.J. Rouse, R.F. Shaw, and M. Wang. 2000. Influence of Atchafalaya River discharge and winter frontal passage on suspended sediment concentration and flux in Fourleague Bay, Louisiana. *Estuarine, Coastal and Shelf Science* 50 (2): 271–290.
Raposa, K.B., K. Wasson, E. Smith, J.A. Crooks, P. Delgado, S.H. Fernald, M.C. Ferner, A. Helms, L.A. Hice, and J.W. Mora. 2016. Assessing tidal marsh resilience to sea-level rise at broad geographic scales with multi-metric indices. *Biological Conservation* 204: 263–275.
Reed, D. 1995. The response of coastal marshes to sea level rise: Survival or submergence. *Earth Surface Processes and Landforms* 20: 39–48.
Rogers, K., N. Saintilan, and H. Heijnis. 2005. Mangrove encroachment of salt marsh in Western Port Bay, Victoria: The role of sedimentation, subsidence, and sea level rise. *Estuaries* 28 (4): 551–559. https://doi.org/10.1007/BF02696066.
Rogers, K., N. Saintilan, A.J. Howe, and J.F. Rodriguez. 2013. Sedimentation, elevation and marsh evolution in a southeastern Australian estuary during changing climatic conditions. *Estuarine, Coastal and Shelf Science* 133: 172–181. https://doi.org/10.1016/j.ecss.2013.08.025.
Rogers, K., K.M. Wilton, and N. Saintilan. 2006. Vegetation change and surface elevation dynamics in estuarine wetlands of southeast Australia. *Estuarine, Coastal and Shelf Science* 66 (3): 559–569. https://doi.org/10.1016/j.ecss.2005.11.004.
Rooth, J.E., and J.C. Stevenson. 2000. Sediment deposition patterns in Phragmites australis communities: Implications for coastal areas threatened by rising sea-level. *Wetlands Ecology and Management* 8 (2): 173–183.
Rovai, A.S., R.R. Twilley, E. Castañeda-Moya, P. Riul, M. Cifuentes-Jara, M. Manrow-Villalobos, P.A. Horta, J.C. Simonassi, A.L. Fonseca, and P.R. Pagliosa. 2018. Global controls on carbon storage in mangrove soils. *Nature Climate Change* 8 (6): 534–538. https://doi.org/10.1038/s41558-018-0162-5.
Schuerch, M., T. Spencer, S. Temmerman, M.L. Kirwan, C. Wolff, D. Lincke, C.J. McOwen, M.D. Pickering, R. Reef, and A.T. Vafeidis. 2018. Future response of global coastal wetlands to sea-level rise. *Nature* 561 (7722): 231–234.
Selvam, V. 2003. Environmental classification of mangrove wetlands of India. *Current Science* 84 (6): 757–765.
Seneviratne, S.I., X. Zhang, M. Adnan, W. Badi, C. Dereczynski, A. di Luca, S. Ghosh., et al. 2021. Weather and climate extreme events in a changing climate.
Smith, J.A.M. 2013. The role of phragmites australis in mediating inland salt marsh migration in a mid-Atlantic estuary. *PLoS ONE* 8 (5): e65091. https://doi.org/10.1371/journal.pone.0065091.
Smoak, J.M., J.L. Breithaupt, T.J. Smith, and C.J. Sanders. 2013. Sediment accretion and organic carbon burial relative to sea-level rise and storm events in two mangrove forests in Everglades National Park. *CATENA* 104: 58–66. https://doi.org/10.1016/j.catena.2012.10.009.
Snyder, C.M., L.C. Feher, M.J. Osland, C.J. Miller, A.R. Hughes, and K.L. Cummins. 2021. The distribution and structure of mangroves (Avicennia germinans and Rhizophora mangle) near a rapidly changing range limit in the Northeastern Gulf of Mexico. *Estuaries and Coasts* 45 (1): 181–195.
Spencer, T., M. Schuerch, R.J. Nicholls, J. Hinkel, D. Lincke, A.T. Vafeidis, R. Reef, L. McFadden, and S. Brown. 2016. Global coastal wetland change under sea-level rise and related stresses: The DIVA Wetland Change Model. *Global and Planetary Change* 139: 15–30.
Stagg, C.L., M.J. Osland, J.A. Moon, L.C. Feher, C. Laurenzano, T.C. Lane, W.R. Jones, and S.B. Hartley. 2021. Extreme precipitation and flooding contribute to sudden vegetation dieback in a coastal salt marsh. *Plants* 10 (9): 1841. https://doi.org/10.3390/plants10091841.
Stagg, C.L., L.A. Sharp, T.E. McGinnis, and G.A. Snedden. 2013. *Submergence vulnerability index development and application to Coastwide Reference Monitoring System sites and coastal wetlands planning, protection and restoration Act projects*. US Department of the Interior, US Geological Survey.
Stallins, J.A., M. Nesius, M. Smith, and K. Watson. 2010. Biogeomorphic characterization of floodplain forest change in response to reduced flows along the Apalachicola River, Florida. *River Research and Applications* 26 (3): 242–260.
Steinmuller, H.E., J.L. Breithaupt, K.M. Engelbert, P. Assavapanuvat, and T.S. Bianchi. 2022. Coastal wetland soil carbon storage at mangrove range limits in Apalachicola Bay, FL: observations and expectations. *Frontiers in Forests and Global Change* 5.
Stone, P.M., and D.E. Walling. 1997. Particle size selectivity considerations in suspended sediment budget investigations. *Water, Air, and Soil Pollution* 99 (1): 63–70.
Thom, B.G. 1982. Mangrove ecology: a geomorphological perspective. In *Mangrove Ecosystems in Australia, Structure, Function and Management*, 3–17. ANU Press.
Twilley, R.R., A.S. Rovai, and P. Riul. 2018. Coastal morphology explains global blue carbon distributions. *Frontiers in Ecology and the Environment* 16 (9): 503–508. https://doi.org/10.1002/FEE.1937.
Wallace, K.J., J.C. Callaway, and J.B. Zedler. 2005. Evolution of tidal creek networks in a high sedimentation environment: A 5-year experiment at Tijuana Estuary, California. *Estuaries* 28 (6): 795–811.
Wang, P., J.D. Adam, J. Cheng, and M. Vallée. 2020. Morphological and sedimentological impacts of Hurricane Michael along the northwest Florida coast. *Journal of Coastal Research* 36 (5): 932–950.
Webb, E.L., D.A. Friess, K.W. Krauss, D.R. Cahoon, G.R. Guntenspergen, and J. Phelps. 2013. A global standard for monitoring coastal wetland vulnerability to accelerated sea-level rise. *Nature Climate Change* 3 (5): 458–465.
Whelan, K.R.T., T.J. Smith, G.H. Anderson, and M.L. Ouellette. 2009. Hurricane Wilma's impact on overall soil elevation and zones within the soil profile in a mangrove forest. *Wetlands* 29 (1): 16–23.
Whelan, K.R.T., T.J. Smith, D.R. Cahoon, J.C. Lynch, and G.H. Anderson. 2005. Groundwater control of mangrove surface elevation: Shrink and swell varies with soil depth. *Estuaries* 28 (6): 833–843.
Williams, G.P., and M.G. Wolman. 1984. *Downstream effects of dams on alluvial rivers*, vol. 1286. US Government Printing Office.
Woodroffe, C. 1993. Mangrove sediments and geomorphology. In *Coastal and estuarine studies*, ed. A.I. Robertson and D.M. Alongi, 7. American Geophysical Union.
Yeates, A.G., J.B. Grace, J.H. Olker, G.R. Guntenspergen, D.R. Cahoon, S. Adamowicz, S.C. Anisfeld, N. Barrett, A. Benzecry, and L. Blum. 2020. Hurricane sandy effects on coastal marsh elevation change. *Estuaries and Coasts* 43 (7): 1640–1657.